



Contents lists available at ScienceDirect

Global and Planetary Change

journal homepage: www.elsevier.com/locate/gloplacha

The contrasting effect of increasing mean sea level and decreasing storminess on the maximum water level during storms along the coast of the Mediterranean Sea in the mid 21st century

Piero Lionello^{a,b,*}, Dario Conte^b, Luigi Marzo^a, Luca Scarascia^b

^a DiSTeBA, Università del Salento, Lecce, Italy

^b CMCC Euro-Mediterranean Center on Climate Change, Lecce, Italy

ARTICLE INFO

Article history:

Received 27 May 2015

Accepted 20 June 2016

Available online xxxxx

Keywords:

Climate change
Mediterranean Sea
Coastline
Sea level
Waves
Extremes

ABSTRACT

The maximum level that water reaches during a storm along the coast has important consequences on coastal defences and coastal erosion. It depends on future sea level, storm surges, ocean wind generated waves, vertical land motion. The future sea level in turn depends on water mass addition and steric contributions (with a thermosteric and halosteric component). This study proposes a practical methodology for assessing the effects of these different factors (which need to be estimated at sub-regional scale) and applies it to a 7-member model ensemble of regional climate model simulations (developed and carried out in the CIRCE fp6 project) covering the period 1951–2050 under the A1B emission scenario. Sea level pressure and wind fields are used for forcing a hydro-dynamical shallow water model (HYPSE), wind fields are used for forcing a wave model (WAM), obtaining estimates of storm surges and ocean waves, respectively. Thermosteric and halosteric effects are diagnosed from the projections of sea temperature and salinity. Steric expansion and storminess are shown to be contrasting factors: in the next decades wave and storm surge maxima will decrease while thermosteric expansion will increase mean sea level. These two effects will to a large extent compensate each other, so that their superposition will increase/decrease the maximum water level along two comparable fractions of the coastline (about 15–20%) by the mid 21st century. However, mass addition across the Gibraltar Strait to the Mediterranean Sea will likely become the dominant factor and determine an increase of the maximum water level along most of the coastline.

© 2016 Elsevier B.V. All rights reserved.

1. Introduction

This paper proposes a practical methodology for computing the maximum water level that will be reached along the coast and estimates how it will change in the future because of global climate change. The study consists in a sequence of three steps that from the outputs of regional climate models i) produce an estimate of the various factors responsible for the water level ii) add the different contributions iii) build indicators of water level maxima, whose values are used for estimating the climate change signal.

The maximum level that water reaches during a storm along the coast is expected to change in future with potentially important consequences on coastal populations and structures (e.g. chapter 5 of IPCC AR5). Results of this study are expected to be relevant for planning coastal and harbor defenses, such as dams, sea walls, breakwaters and structures such as jetties and docks. The analysis is applied to the Mediterranean sea leading to an estimate of future maximum water level

along its whole coastline, whose vulnerability has been recognized since long time (e.g. Nicholls and Hoozemans, 1996).

In spite of the relevance of the issue, it appears that no study has so far attempted a comprehensive estimate of the maximum water level including the superposition of the different relevant factors: mass addition, changes of density (steric effects), vertical land motion, changes of storm surges and of wind generated surface waves. All these factors need to be estimated at sub-regional scale as they are characterized by a large variability in space and time.

The mean sea level of the Mediterranean Sea has shown, in the recent past, substantial deviations from the global values at decadal time scales. In the period 1960–1990 the mean Mediterranean sea level actually decreased, mainly because of a persistent positive anomaly of sea level pressure (Tsimplis et al., 2005; Marcos et al., 2011a). Later, during the 1990s, it increased at a speed greater than the global one, and subsequently stopped from 2002 onwards (Marcos et al., 2011a, 2011b, 2011c). This behavior can be due to mass exchanged with the Atlantic across the Gibraltar strait, to change of volume because of change of temperature and salinity, or, more in general to a combination of both. A mean flow of mass across Gibraltar can be the consequence of ice

* Corresponding author at: DiSTeBA, Università del Salento, Lecce, Italy.
E-mail address: piero.lionello@unisalento.it (P. Lionello).

melting, which increases globally the mass of the oceans, or/and of changing sea level pressure distribution over the North Atlantic and Mediterranean regions. Calafat et al. (2010) have estimated the mass contribution to Mediterranean Sea level variability for the period 1948–2000. They found that the mass content of the Mediterranean basin has increased at a rate of 0.8 ± 0.1 mm/yr for the period 1948–2000 and that it increases up to 1.2 ± 0.2 mm/yr if the effect of the atmospheric surface pressure is removed. The steric contribution has been estimated to contribute about 20% of sea level variance (Tsimplis et al., 2008) in model simulations and it is clearly smaller than the effect of mass addition, which is the real cause of the observed increase of the Mediterranean sea level (Jordà and Gomis, 2013a, 2013b). Its estimate, which is affected by the uncertainty of oceanographic observations containing dubious records and holes during the 20th century, indicates that a small steric sea level increase could eventually have been driven mainly by warming of the upper waters (Tsimplis and Rixen, 2002). However, concerning long-term trends (1960–2000), even the sign of the thermosteric component is uncertain and ranges from -0.06 to $+0.09$ (Jordà and Gomis, 2013b). Halosteric trends are negative for all products, but the magnitude and spatial patterns provided by available hydrographic datasets are statistically inconsistent among them.

The future evolution of Mediterranean Sea level is uncertain. Some regional studies have focused on the steric contribution. Marcos and Tsimplis (2008) have used a large set of global climate models (GCMs) for computing the steric effect on Mediterranean sea level. They have found a large spread among model results (from -22 to 31 cm at the end of the 21st century), with density increase (due to the projected increase of salinity) compensating the thermosteric expansion (due to the projected warming) in some models. These estimates have been recently reconsidered using the CIRCE simulations (Gualdi et al., 2013), which provided estimates of the 2021–2050 mean steric sea level rise with respect to the reference period (1961–1990) in the range from 2 to 7 cm. All these estimates are valid under the hypothesis that the total water mass in the Mediterranean will not change, which seems dubious if salinity will change. An attempt to consider the total sea level using a statistical model has been done by Scarascia and Lionello (2013), but only at sub-basin scale for the Adriatic Sea under the A1B scenario, where they estimated a total sea level rise in the range from 14 cm to 49 cm at the end of the century. The future effect of the atmospheric mechanical forcing has been estimated by Jordà et al. (2012) suggesting a sea level decrease in winter, with trends of up to -0.8 ± 0.1 mm/year in the central Mediterranean under the A2 scenario, and a small increase in summer (0.05 ± 0.04 mm/yr).

Marine storminess in the Mediterranean region is associated with a well-defined sub-branch of the mid-latitude storm track and a consensus on a decrease of its intensity has progressively emerged in the literature (Lionello et al., 2006, 2008a; Lionello and Giorgi, 2007; Zappa et al., 2013), which is especially evident considering the RCP8.5 scenario in the latter study. Correspondingly, significant wave height and storm surges are projected to decrease (Lionello et al., 2008b; Marcos et al., 2011b; Conte and Lionello, 2013). For both wave and surge maxima the value of the reduction varies depending on the basin in the range from 2% to 5% in the period 2021–2050 with respect to 1971–2000 for the A1B scenario.

This study differs from previously published studies because it aims at computing the maximum level that water can reach during a storm considering simultaneously various factors, that were considered separately in previous studies: storm surges, ocean wind generated waves, steric effects on sea level. Further its output is designed in such a way to focus on the coastline (Fig. 1a), where effects of water level maxima are most important and it is essential to adapt to their eventual future variation. The goal is to assess the climate change effect on marine storminess along the coast of the Mediterranean Sea in the next decades. A multi-model approach is adopted by using the forcing fields provided by a new generation of coupled regional atmosphere-ocean models that were developed in the CIRCE FP7 project (Gualdi et al.,

2013). However, this study does not include land vertical motions (which need a completely different set of models and information) and the effect of mass addition caused by melting of polar and continental ice caps, which is an essential, but complicated issue in its own (Church et al., 2013).

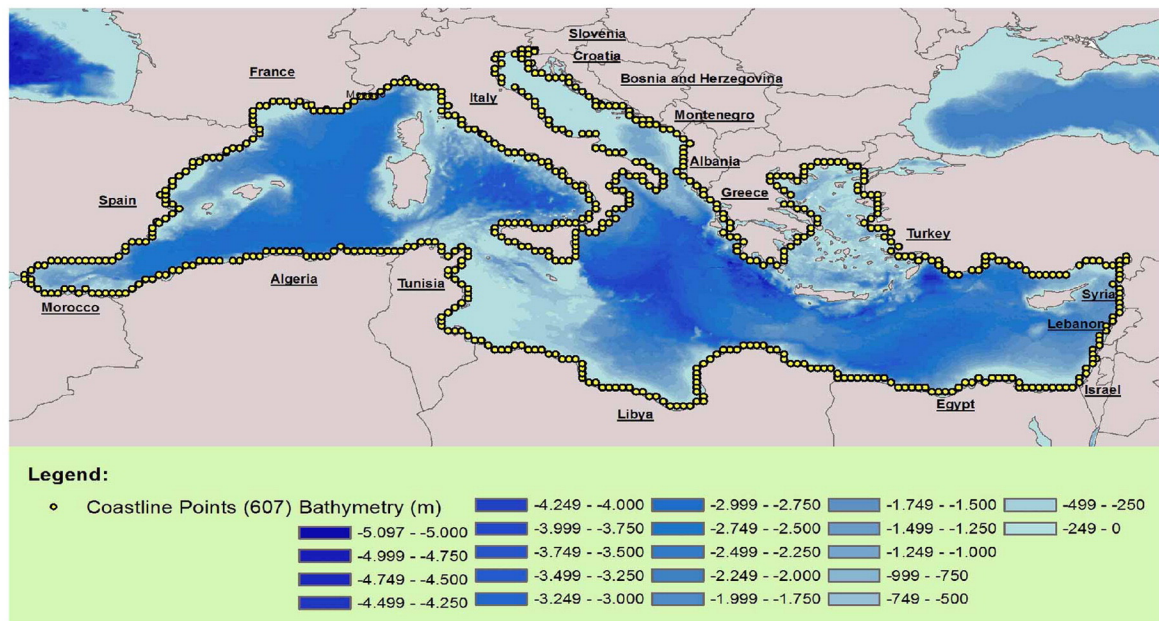
The organization of this paper reflects the different factors that are included in this analysis. Section 2 (Data and methods) lists the climate model projections (Section 2.1) providing the sea level pressure (SLP) and surface wind fields and describes briefly the models used for computing the surge levels and the wind wave spectra (Section 2.2). The following two Sections (2.3–2.4) describe how the contribution of wind generated waves and steric effects to the maximum water level are computed. Section 2.5 describes the indicators that are used to describe climate change. Section 3 analyzes the results of the simulations considering first separately the role of waves (Section 3.1) and surges (Section 3.2), and then adding them to compute the maximum water level reached by wave crests during a storm. Initially the analysis considers the average annual maximum water level. Results for other indicators are described in Section 3.4 (the average 10 independent annual maxima, the 5 and 50 years return values) and in Section 3.5 (storm duration). Steric effects are described in Section 3.6. The discussion (Section 4) describes the net effect of storminess (waves and surges) and steric effects on the maximum water level. The study is summarized in the conclusion Section 5.

2. Data and methods

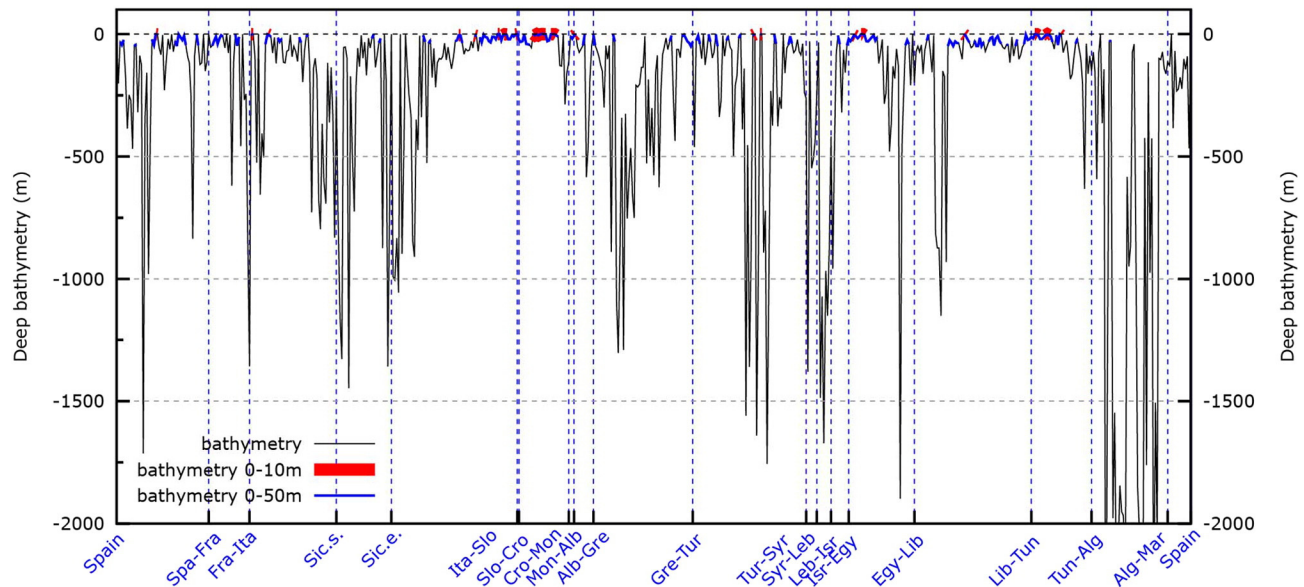
2.1. Climate model projections

Input data for this analysis are provided by a set of climate simulations that have been produced within the CIRCE fp6 project (Climate Change and Impact Research: the Mediterranean Environment) and cover the period 1951–2050 under the A1B emission scenario (Gualdi et al., 2013). Seven simulations have been considered, labeled CMCC-LR, CMCC-HR, MPI, ENEA, CNRM, IPSL3, IPSL2. All simulations except CMCC-HR are carried out with coupled atmosphere ocean models including a high resolution model of the Mediterranean Sea circulation.

- The CMCC-LR (Euro Mediterranean Centre for Climate Change Low Resolution) datasets produced using the global climate model CMCC-Med, whose atmospheric component is ECHAM5 in its T159 configuration (~ 150 km) and ocean component is OPA8.2 at 2° resolution. Over the Mediterranean basin ECHAM5 is fully coupled with NEMO-MFS at a 6.7 km resolution (Oddo et al., 2009).
- The CMCC-HR (Euro Mediterranean Centre for Climate Change High Resolution) datasets produced using the CMCC-CLM Regional Climate model downscaling of the CMCC-LR simulation and it represents its dynamical downscaling to an horizontal grid resolution of $0.12 \times 0.12^\circ$.
- The MPI (Max Plank Institute-Germany) dataset, which is produced using REMO (REgional Model) which is a dynamical downscaling of the CMCC-LR model at a spatial resolution of $0.22 \times 0.22^\circ$ coupled to the Max-Planck-Institute for Meteorology ocean model (MPI-OM). The boundary conditions are extracted from CMCC-LR simulation (Elizalde et al., 2010).
- The ENEA (Italian National agency for new technologies, Energy and sustainable economic development) dataset, which is produced using the RegCM3 regional atmospheric model coupled to the MITgcm model in the Mediterranean Sea (Carillo et al., 2012). This dataset is a downscaling of ECHAM5-MPIOM at resolution of 30 km for the atmospheric component and $1/8^\circ$ for the ocean component.
- The CNRM (Centre National de Recherches Météorologiques - MétéoFrance) dataset, which is produced using the ARPEGE atmospheric circulation model (Déqué and Piedelievre, 1995), whose stretched grid reaches a 50 km resolution over Europe-Mediterranean-North Africa) coupled to OPA9 at 2° resolution for the global



(a) - Coast Grid Points / Bathymetry map



(b) - Coast Grid Points (National and Regional Borders)

Fig. 1. a (top) The Mediterranean Sea bathymetry with the coastal grid points (yellow dots) where the climate change analysis is performed. In Fig. 1b (bottom) coastal sea points of Fig. 1a are ordered clockwise from Spain (left margin of the x-axis) to Morocco (right margin of the x-axis). Country national borders are marked to help locating the different parts of the Mediterranean coastline. (Sic.s. and Sic.e. denote the first and last point of the Sicilian coastline). Fig. 1b shows the value of the depth in the grid cell closest to the coast of the ETOPO1 global, integrated bathymetric–topographic, digital elevation model with cell size of 1 arc-minute (Amante and Eakins, 2009). The parts where the depth is less than 10 m are marked red, less than 50 m are marked blue. (For interpretation of the references to colour in this figure legend, the reader is referred to the web version of this article.)

circulation and to NEMO-MED8 (1/8° resolution) for the Mediterranean Sea circulation (Somot et al., 2008).

- The IPSL3 (Institute Pierre Simon Laplace) dataset, which is computed by the LMDZ RCM (30 km resolution) coupled to MEMO-MED at 1/8° resolution in the Mediterranean Sea. It is a dynamical downscaling of a global simulation carried out using LMDZ GCM (300 km resolution, e.g. Li et al., 2012) as atmospheric component coupled to OPA9 at 2° resolution as ocean circulation component (Li, 2006)
- The IPSL2 dataset, which is produced by the same models as IPSL3, but adopting a two way coupling for the nest, that is four models - two atmospheric (global and regional) and two oceanic (global and regional) - have been run together allowing the results at regional

scale to feedback on the global models. Therefore, IPSL2 and IPSL3 are two independent simulations, carried out with a different model setup.

Results of these 7 simulations have been used for 3 sets of computations: i) the surface wind fields have been used for driving the wave model WAM and producing projections of the wave fields for the whole Mediterranean Sea; ii) the SLP (Sea Level Pressure) and wind fields have been used for driving the hydro-dynamical shallow water model HYPSE (Hydrostatic Padua Sea Elevation model) and producing sea level projections; iii) the sea temperature and salinity fields have

been used for computing sea water density and the steric sea level variation.

2.2. Storm surge and wind waves projections

Computation of storm surges have been carried out using the Hydrostatic Padua Surface Elevation (HYPSE) model, which is a two-dimensional model based on depth averaged currents (see Lionello et al., 2005 for a description of the model). HYPSE has been implemented on a 168×82 lon-lat grid, which covers the whole Mediterranean sea with a 0.2° steps in latitude and longitude (Fig. 1a). Seven simulations have been produced forcing HYPSE with the SLP and surface wind fields of the seven climate models described in Section 2.1. Therefore seven projections of SL evolution have been made available. These set of data has already been used in Conte and Lionello (2013) for analyzing the change of large surges along the coast of the Mediterranean Sea. Validation of the model has been performed comparing the maxima of a model hindcast to 21 tide gauges and showed that the present spatial variability of surge extremes and the shape of their mean annual cycle are adequately reproduced. Further, time correlation has acceptable values in the months when the highest surges occur. Readers can find in Conte and Lionello (2013) a detailed discussion.

The simulations of the wind wave fields have been carried out using WAM (WAMDI group et al., 1988). WAM is a widely used model, which solves the wave energy equation for the components of the wave spectrum. Here it has been implemented on a grid at 0.25° resolution, resolving the spectrum using 12 directions and 25 frequencies. This implementation has already been used and validated in previous studies that analyzed present variability (Lionello and Sanna, 2005) and climate change projections (Lionello et al., 2008a, 2008b).

2.3. Computation of the wave contribution to the maximum water level

Here we are considering the maximum level reached during a storm by the wave crests. This problem has been addressed first in the theory of the joint distribution of wave heights and periods by Longuet-Higgins (1975) under the assumption of a narrow band spectrum (see Goda, 1978, 2008 for reviews of the accuracy of this theory). Considering the ratio $\beta = h_{1/p} / h_{1/3}$ of the height of the wave crest $h_{1/p}$ (exceeded with a $1/p$ frequency) to the significant wave height $h_{1/3}$ (which is the quantity provided by wave models), the Rayleigh distribution provides number such as $\beta = 1.51, 1.66, 1.86$ for $p = 100, 250, 1000$, respectively. Here we use $\beta = 1.8$ with the intent of giving an estimate of the highest waves during a storm whose duration is a few hours and following Goda (1978). This approximation does not account for the deviation of the windsea spectrum from the narrow band hypothesis, but it is usually considered sufficiently accurate to be adopted by practitioners.

The problem is further complicated by the limitation imposed by wave depth on the wave height distribution within the surf zone, when the wave height becomes comparable with the water depth. A well-known and widely referred solution to this problem can be found in Battjes and Janssen (1978), who consider a threshold coefficient k such that wave breaking occurs when $h_{max} = kD$, where D is the water depth, originally proposing $k = 0.8$. Successively, it has been shown that the value of k varies with the slope of the sea bottom (Battjes and Groenendijk, 2000), with a minimum about $k = 0.55$ for a flat bottom (Nelson, 1994) to values close to 1.0 when the sea bottom is very steep. Fig. 1b shows the value of the depth in the grid cell closest to the coast of the ETOPO1 global, integrated bathymetric–topographic digital elevation model, with cell size of 1 arc-minute. (Amante and Eakins, 2009). The short parts of the coastline where offshore depth values are less than 10 (and 50) meters are marked red (and blue). Therefore, deep limited breaking could affect the results of this study only at very few coastal points.

In practice for considering the maximum water level here we assume $h_{max} = 1.8 h_{1/3}$ and, therefore, add $a_{max} = 0.9 h_{1/3}$ representing

the maximum wave amplitude to the change of sea level produced by the storm surge and steric effects. This further implies that this study ignores the asymmetry of the nonlinear wave profile, where the deviation from the mean sea level is larger in correspondence with the crests than with the troughs.

2.4. The computation of the steric effect on sea level

The specific volume of water depends on temperature and salinity. If the total mass is constant, an increase of temperature/salinity implies an expansion/contraction of the water column and, correspondingly, sea level increase/decrease. These two effects are called thermosteric expansion and halosteric contraction. However, the assumption of constant mass is clearly difficult to be maintained, especially for changes of salinity, which are necessarily related to a change of the mass budget of the Mediterranean Sea due to changes of evaporation, precipitation or river runoff. Therefore, how to use the steric sea level changes that are computed using temperature and salinity produced by regional ocean circulation models is controversial. Clearly temperature and salinity 3-dimensional distributions do not contain information sufficient for computing the change of sea level (Jordà and Gomis, 2013a, 2013b) and it is necessary to include information on the spatial distribution of mass change, which depends also on interaction with the Atlantic Ocean across the Gibraltar Strait. (see Jordà and Gomis, 2013a, 2013b for a detailed discussion). Computations that have been done in the past, producing maps of sea level change (e.g. Marcos and Tsimplis, 2008) or computing average values over the whole Mediterranean Sea (e.g. Gualdi et al., 2013) should, therefore, not be considered really representation of actual future sea level rise. In this study, we share these limitations, because we have information nor on internal redistribution of mass within the Mediterranean Sea, neither on its addition across the Gibraltar Strait. In this study, mass has, therefore been considered constant, except for the effect of salt addition, which has been included, but it is actually small in the analyzed simulations. The change of water volume has been computed separately in six sub-basins composing the Mediterranean Sea (western Mediterranean, Tyrrhenian Sea, Adriatic Sea, Central Mediterranean, Aegean Sea, Levantine basin) and the consequent change of sea level has been assumed uniform within each of them.

It is stressed that this study misses completely an independent estimate of the mass contribution to the Mediterranean Sea level from the Atlantic Ocean. This has been estimated in the range 0.8 to 1.0 mm/year during the second half of the 20th century (Calafat et al., 2010) and identified to be the main source of uncertainty in future sea level change at sub-regional scale (Scarascia and Lionello, 2013). The role of this missing information, which has been shown to be the largest contribution to recent Mediterranean sea level rise (Marcos et al., 2011a, 2011b, 2011c; Jordà and Gomis, 2013a, 2013b), is discussed in Section 4.

2.5. Indicators of climate change

This study aims at analyzing the changes of water level extremes, which are relevant for overtopping coastal defenses. As anticipated this is discussed considering three contributions: the change of sea level due to the combined action of sea level pressure and winds that occurs during storm surges, the maximum height of the wave crests, the steric effect that expands or contracts the water column. These three effects can be considered together adding steric sea level change, storm surge and amplitude of the wave. However, as described in Section 3, they will also be discussed separately in order to assess their relative importance.

As this study is focalized on the max water level at the coast, results are analyzed in the coastal points of the HYPSE grid shown in Fig. 1a. Results of WAM and of the steric computation are linearly interpolated to this set of 607 points, so that all values are made available exactly in the same set of locations. In the figures showing the results the coastal grid

points have been ordered clockwise along the whole coast of the basin, which is eastwards along the European northern coast of the Mediterranean and westwards along the African southern coast. The analysis has considered time series of 3-hourly values for both wave height and storm surges.

Evaluation of the climate change signal in climate projections is based on comparing the values of two 30 year-long periods: 1971–2000, representing the past (reference), and 2021–2050 representing the future.

Different indicators are considered to describe maxima: $\text{ind1}_{1971-2000}$ and $\text{ind1}_{2021-2050}$, which is the average of the annual maxima in the two periods, $\text{ind10}_{1971-2000}$ and $\text{ind10}_{2021-2050}$, which is the average of the 10 largest maxima in the two periods, $\text{rv5}_{1971-2000}$ and $\text{rv5}_{2021-2050}$, which is the 5-year return value, and $\text{rv50}_{1971-2000}$ and $\text{rv50}_{2021-2050}$, which is the 50-year return value. These indicators can be computed separately for the wave amplitude (wa), for the storm surge level (ss) and for the water level (wl), which is the sum of the two previous contributions. The variable that is considered is denoted by the characters “wa”, “ss” and “wl” before the name of the indicator. In other word indicators labels are composed of three parts. The initial two letters denote the variable, the remaining part of the name the type of indicator and the subscript denotes the considered period. For instance, $\text{w1ind10}_{1971-2000}$ is the average of the 10 largest annual maxima water level in the period 1971–2000 and $\text{warv5}_{2021-2050}$ is the 5 year return value of the wave maximum amplitude in the period 2021–2050. Climate change signal is computed as percent variations of the indicators, that is the difference between the two periods normalized with the present value. Positive values indicate a future increase of indicators.

Steric increase is computed as difference between average values in the two “present” and “future” periods and its relevance is discussed separately.

Three climate simulations (CMCC-LR, CMCC-HR, MPI), are related and tend to reproduce the same sequence of large scale synoptic events, while the remaining four simulations (ENEA, CNRM, IPSL2, IPSL3) are independent., though it is difficult to use a clear criterion for IPSL2 and IPSL3. Therefore, weights are assigned with the same criterion that was used in Conte and Lionello (2013), with the three simulations CMCC-LR, CMCC-HR, MPI having a total weight 1/5 (composed of 1/10 for CMCC-LR, and 1/20 for CMCC-HR and MPI). All other simulations have a weight equal to 1/5. As CMCC-HR includes no ocean model, when computing the steric sea level the weight of MPI is increased to 1/10. In all analysis, statistical significance is attributed when the climate change signal is larger than the inter-model standard deviation.

3. Results

Here we discuss first separately the changes of annual maxima of storm surge and of wave amplitude. Then the two factors are superimposed to assess the changes of the annual maximum water level during a storm. The discussion is also extended to indicators of maximum water levels with different likelihood: the average of the 10 highest water level, the 5 and 50 year return time values of the maximum water level. When considering the 10 highest water levels, only maxima separated by a minimum interval (3 days) have been considered. The relevance of the steric effect is discussed separately.

3.1. Analysis of the annual maximum wave amplitude

On the basis of the method described in Section 2.3, here we discuss the maxima of the wave amplitude. Fig. 2a shows the value of $\text{w1ind1}_{1971-2000}$ along the Mediterranean coast according to the different models and their weighed ensemble mean. There is a substantial consensus among models on the geographical distribution of maxima of wave amplitude, which is consistent with the open sea climatology (e.g. Lionello et al., 2008a, 2008b) and the track of marine storms in

the Mediterranean (Lionello et al., 2006). Large values occur where the coastline is exposed to the action of a strong wind with a long fetch, such as the southern coast of the Tyrrhenian Sea (north coast of Sicily and western coast of south Italy), the northern coast of Africa, the coasts of Egypt, Libya and Algeria.

The lower panel shows the percent climate change of the w1ind1 indicator. Individual models do not always agree and the same model can have substantially different climate change values in different parts of the coastline. However, the weighted ensemble mean shows a negative signal (meaning a future reduction of maximum wave amplitude), which is consistently significant along most of the Mediterranean coastline with values between 2% and 5%.

3.2. Analysis of the annual maximum surge levels

Fig. 3a–b show the value of $\text{ssind1}_{1971-2000}$ and its percent climate change along the Mediterranean coast according to the different models and their weighed ensemble mean. Results, which are consistent with Conte and Lionello (2013), show the spatial distribution of storm surge maxima (the largest values occur in the North Adriatic Sea and Gulf of Gabes) and their wide spread reduction in the future. Reduction of maximum wave amplitude and storm surge are consistent, but not similar in detail. Differences are due to their different response to changes in storminess. In deep water storm surge levels scale with the gradient of the mean sea level atmospheric pressure and in shallow water they scale with the wind stress, while wave amplitude scales with the wind stress both in deep and shallow water. For storm surge maxima (as well as for waves) climate change signal differs in detail among models, but the ensemble mean reveals a substantial consensus on a reduction of order 5% along most of the Mediterranean coastline. The climate change signal for storm surge maxima is extensively discussed in Conte and Lionello (2013).

3.3. Annual maximum water level increase during a storm

During a storm the maximum water level results from the superposition of waves and storm surge. Besides Figs. 2 and 3, describing separately wave amplitude and storm surge maxima, a further figure could be produced describing the water level w1ind1 obtained by the superposition of the two processes for each model simulation. However, the two panels of this figure would be almost identical to the respective figures with wave amplitude maxima (Fig. 2a–b), because the contribution of storm surge is substantially smaller than that of waves.

Fig. 4 compares w1ind1 , ssind1 and w1ind1 showing only the weighed ensemble mean of the simulations and confirms that the two indicators w1ind1 and w1ind1 have an almost identical distribution along the coastline, which results in a very similar climate change signal. The black line of Fig. 4a shows that the percent contribution of the storm surge to the maximum water level (given by the ratio $100 \cdot (\text{w1ind1}_{1971-2000} - \text{w1ind1}_{1971-2000}) / \text{w1ind1}_{1971-2000}$) is rather small along most of the coastline but in the northern Adriatic and the Gulf of Gabes, where it is almost 20%. Therefore, wave amplitude and its change are much more important than storm surge and storm surge changes for the water level maxima and overtopping coastal defenses. Fig. 4b shows the climate change of the weighed ensemble mean for the w1ind1 , w1ind1 and ssind1 indicators. It shows that climate change signals of waves and surges coincide over most of the coastline (e.g. the coast of the Adriatic Sea, the coast of Libya and of Algeria), but the decrease of storm surge maxima is larger than that of wave amplitude maxima along some deep parts of the coastline (the eastern coast of Spain, the Ionian and Aegean Sea coastline).

3.4. Other indicators of extreme water levels

Indicators of extremes that are weaker (more frequent) and stronger (more rare) than the annual maximum water level are shown in Fig. 5

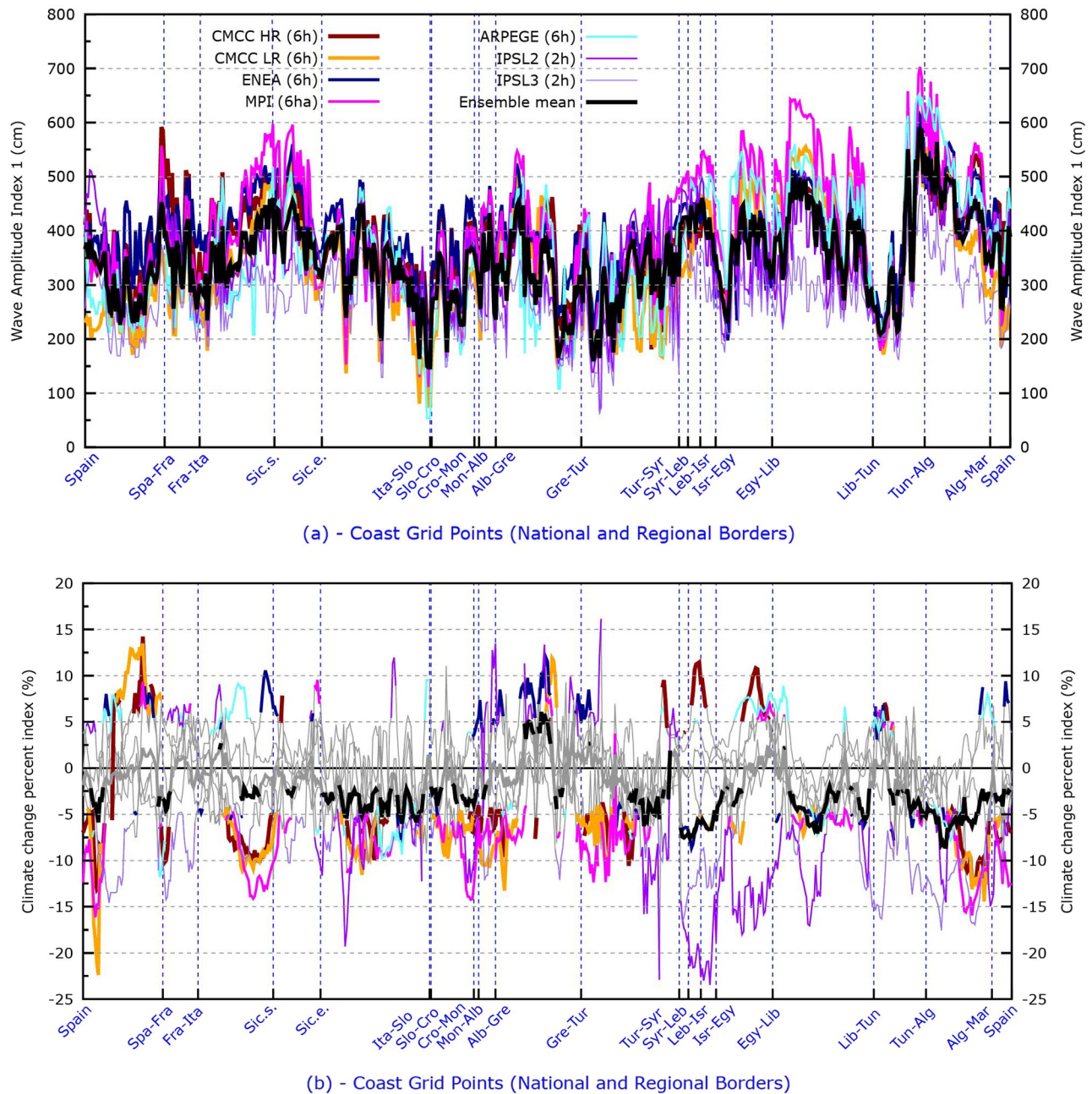


Fig. 2. a (top): distribution of the $w_{\text{aind1}}_{1971-2000}$ indicator in the individual model simulations (thin colored lines). Different colors are used to denote different simulations (labels are annotated in the figure). The weighted ensemble mean is shown by the thick black line. Fig. 2b (bottom): percent climate change index for $w_{\text{aind1}}_{2021-2050}$ with respect to $w_{\text{aind1}}_{1971-2000}$. Thick colored lines represents statistically significant values of each simulations. Thick gray line is the weighted ensemble mean. The thick black line shows significant values of the weighted ensemble mean percent climate change index.

shows, which, besides w_{ind1} , includes also results for w_{ind10} , w_{lr5} , w_{lr50} . Spatial variability in the present climate (Fig. 5a) is similar for all these 4 indicators. The climate change signal (Fig. 5b) is similar for w_{ind10} , w_{ind1} , w_{lr5} , but there are differences in the fraction of the coastline along which it is statistically significant. Future reduction is significant practically everywhere considering w_{ind10} , and along a progressively decreasing fraction of the coastline considering w_{ind1} and w_{lr5} . The climate change of w_{lr50} has a more irregular distribution than that of other indicators and presents a large significant increase along the coast of Spain and Greece. Therefore, extremes are mostly expected to decrease in the next decades, but fifty year return levels

(w_{lr50}) might actually increase along some parts of the Mediterranean coastline.

3.5. Storm duration

The total duration of the storms is another indicator of the stress exerted on the coastal structure and environment. Here the duration of a marine storm is defined as the period during which the maximum water level is larger than the threshold given by the local value of the 95th percentile of the 3-hourly water level ($w_{\text{l95}}_{1971-2000}$) in the reference period 1971–2000. The total

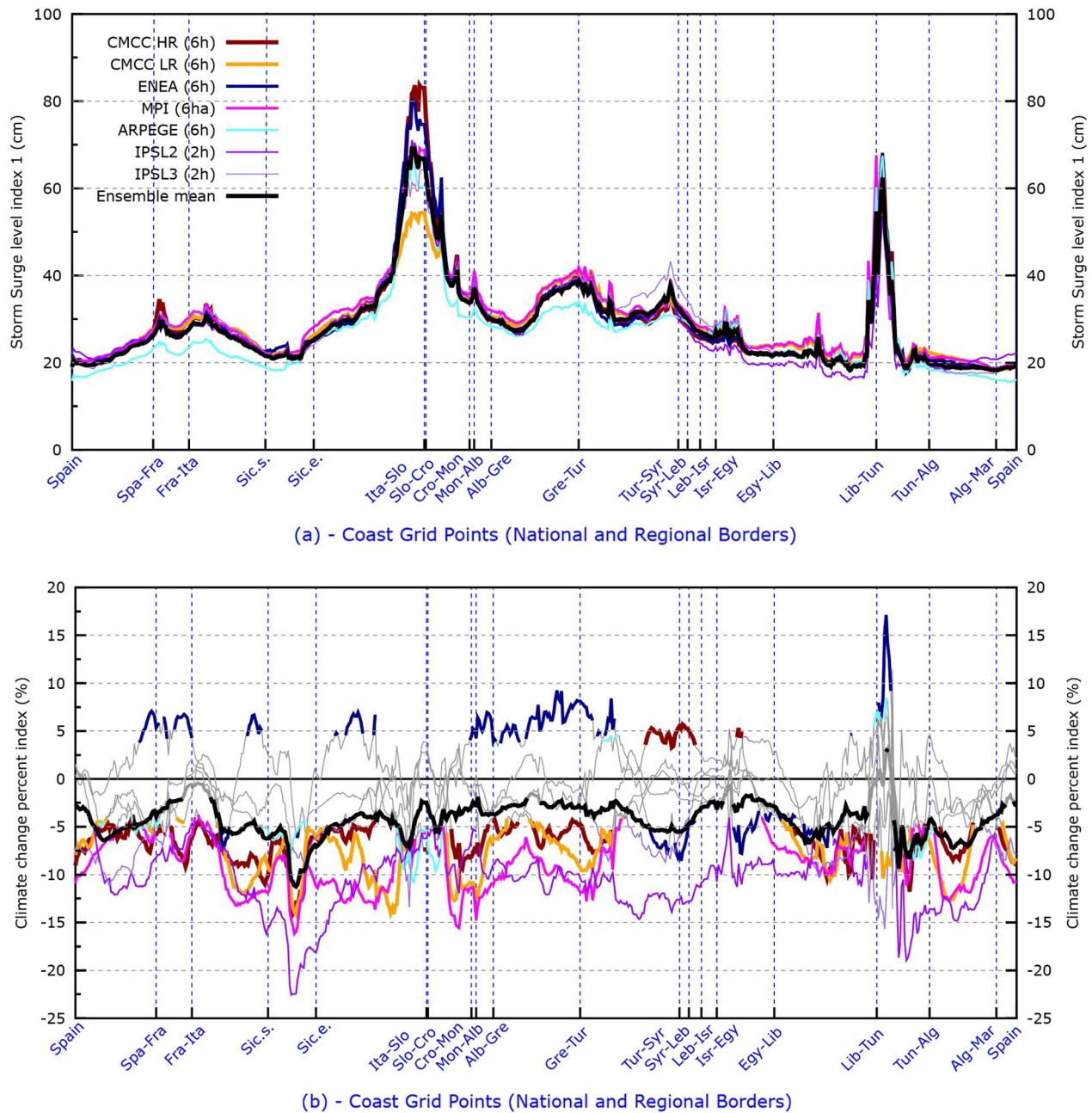


Fig. 3. a and b same as Fig. 2a and b, respectively, except it shows the ssid1 values and their percent climate change.

duration of marine storms is computed by counting the number of steps in the period 2021–2050 with water level above $wl95_{1971-2000}$. Fig. 6 shows the decrease of the total duration of storms (hours) in the 2021–2050 period with respect to the reference period. Since, according to the definition, the annual average total duration of storms in the reference period is approximately 18 days, the reduction shown in figure is larger than 10%.

3.6. Steric effects

Fig. 7 shows the change of the steric sea level. Its value is uniform along large parts of the coastline, since the steric level variation is computed considering average values in six different sub-basins (as it is described in Section 2.4). Only average annual values are

shown in Fig. 7, because, though the steric height (particularly the thermosteric component) has a non-negligible annual cycle, its variations between the average values in the 2021–2050 and 1971–2000 periods do not depend appreciably on the month. Most of the climate change signal is due to the thermosteric component and to the increase of temperature of the water column. Halosteric effects have a small role on sea level changes, because though the increased future water deficit in the basin would tend to increase its salinity, the inflow of fresh water across the Gibraltar strait has a strong compensating action in these model simulations. Therefore, with the exception of the ARPEGE model results, Fig. 7 shows a tendency of the water column to expand, because of warming sea water temperature, with values in the range from 4 cm (in the shallow Adriatic Sea) up to 8 cm in other basins for the ensemble mean. Uncertainty

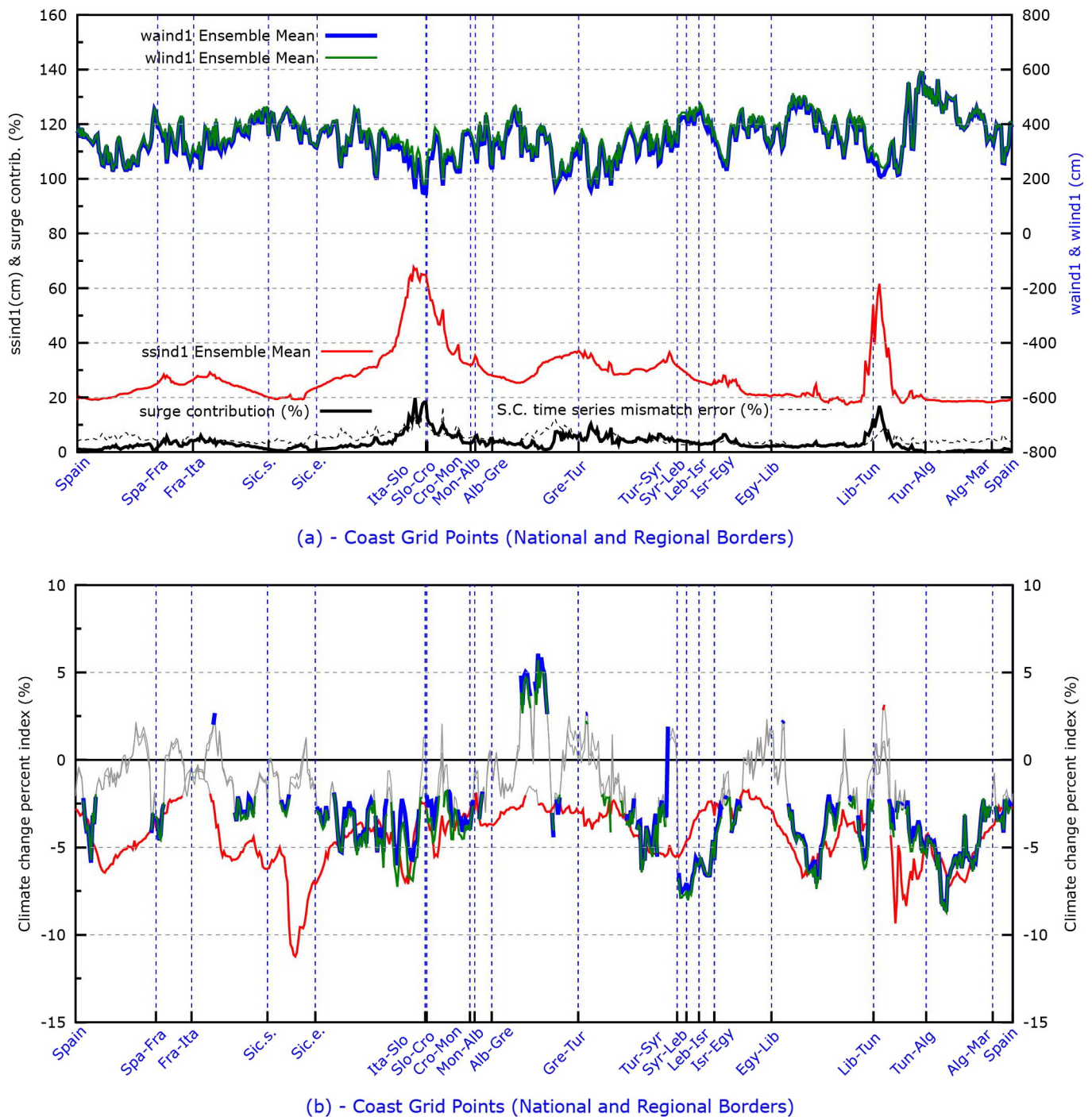


Fig. 4. a (top): present distribution of water level maxima w_{ind1} 1971–2000 (green line) and wave amplitude maxima w_{ind1} 1971–2000 (blue line, units along the right axis of the panel) and storm surge maxima ss_{ind1} 1971–2000 (red line, units along the left axis of the panel). The black line shows the percent contribution of storm surge maxima to the maximum water level. The dashed line shows the percent systematic error when computing the maximum water level by adding w_{ind1} 1971–2000 and ss_{ind1} 1971–2000 instead of analyzing the time series obtained adding the corresponding 3-hourly values. Fig. 4b (bottom): climate change signal for w_{ind1} , ss_{ind1} , w_{ind1} . In both panels only the weighted ensemble mean is shown. (For interpretation of the references to colour in this figure legend, the reader is referred to the web version of this article.)

is large especially in the Eastern Mediterranean and particularly in the Levantine basin, where intermodal differences cover the range from -2 to 20 cm.

4. Discussion

This study shows that along the coast of the Mediterranean Sea waves are the main factor responsible for changes of maximum water

level during a storm, while the storm surge contribution is less important. This depends on the substantial difference of magnitude between the two phenomena. Maxima are in the range from 2 to 6 m for the wave amplitude, and from 20 to 60 cm for surges, so that there is almost one order of magnitude difference between the respective contributions to the maximum water level. The largest percent contribution (about 20%) of the storm surge to the maximum water level occurs at the coast of the Northern Adriatic Sea and Gulf of Gabes. Along other

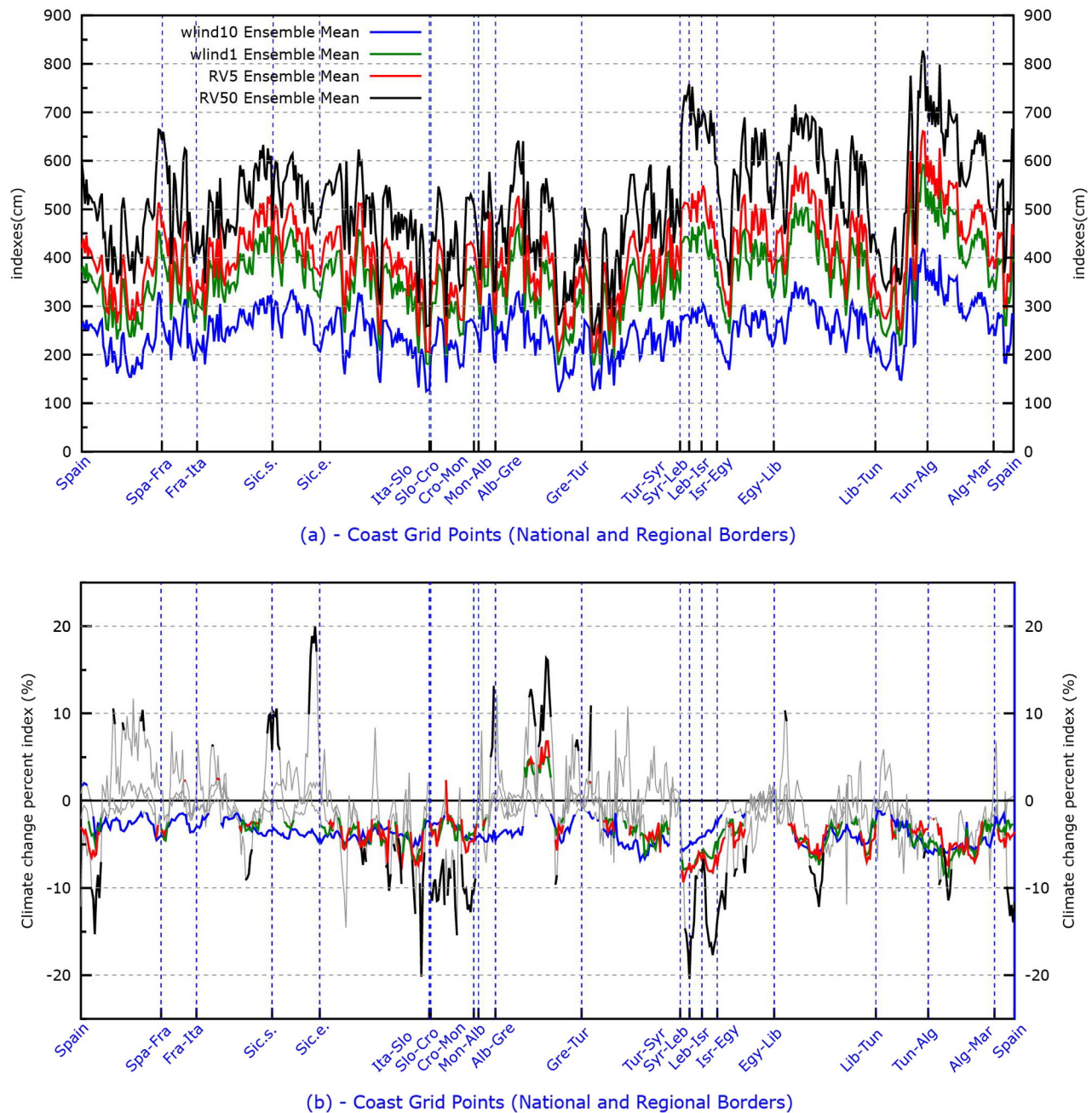


Fig. 5. a (top): present distribution of water level annual maximum indicators: wlv5_{1971–2000}, of the 10 largest maxima indicator wlv10_{1971–2000}, of the 5 and 50 year water level return values wlv5_{1971–2001} and wlv50_{1971–2000}. Fig. 5b (bottom): corresponding climate change signal. In both panels only the weighted ensemble mean is shown. Thick parts of the lines in Fig. 5b denote statistically significant values.

stretches of the coastline its contribution to the climate change signal is small, so that the change of the maximum water level is very similar to that of the maximum wave amplitude.

In this study, when computing wlv10, the annual maxima of water level are extracted from the 3-hourly time series that are obtained adding time series of wave amplitude and sea level values. Otherwise, a water level maxima could be computed adding directly maxima of wave amplitude and of storm surge. Results are different because maxima of surges and of wave amplitude do not coincide in time during the same storm and, further, characteristics of storms producing extreme wave heights and surge levels are different. In practice, adding wlv10 and wlv10 would produce a systematic overestimation of annual water level maxima. The dashed line in Fig. 4a shows the relevance of this error as percent of the actual wlv10_{1971–2000} indicator, with

values in the range 5–10%, which may be relevant for practical applications.

In Section 3 two contrasting factors affecting the maximum water level that will be reached during a storm at the coasts of the Mediterranean Sea have been evaluated. On one hand, in the future, reduced storminess will produce lower waves and surges than now. On the other hand, the net steric effect (producing an expansion of the water column) will shift the whole probability distribution of sea level towards high values, therefore increasing the probability of large water levels during storms. Here we discuss what is the net effect of the superposition of these two factors.

While Section 3 has mainly considered percent variations of the water level, in this discussion we estimate the actual variation (dimensional) of water level maxima. Changes of wlv10, wlv5, wlv50,

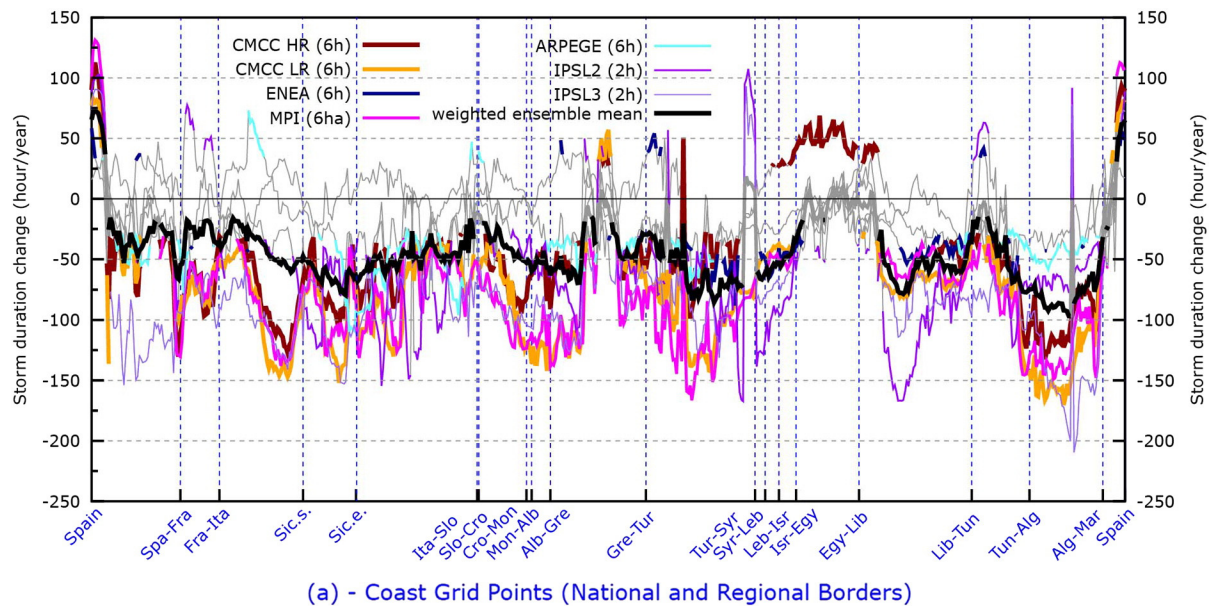


Fig. 6. same as Fig. 2b except it shows the change of the storm duration indicator in hours/year.

wlrv50 are estimated by applying the ensemble mean percent change to the present ensemble mean distribution. The steric change (shown in Fig. 7) has been added to these values obtaining estimates (Fig. 8) of the change of maximum water level reached during a storm with respect to the present situation, accounting for both steric effect and change of storminess. Fig. 8 shows that along a large fraction of the Mediterranean coastline the reduction of storm intensity will compensate for the thermosteric effect, so that the maximum water levels will only marginally change for extremes up to the five year return level. In fact, changes of wlv1, wlv10, wlv5 are significant in very few points and remain significantly negative in the Adriatic Sea and along the coast of the Middle East even including the steric effect on sea level rise. Considering wlv50, that is a longer return time, the fraction of coastline with statistically significant positive (negative) climate change increases (decreases). Increases of wlv50 are reinforced by

the thermosteric expansion and are evident at the coast of Spain, at the coast of Sicily and along both the Ionian and Aegean sectors of the coast of Greece. However, in spite of the contrasting thermosteric expansion, significant reduction of wlv50 is present in the Adriatic Sea and at the Middle East coast of the Levantine basin.

Mass addition is a further essential contribution that needs to be included and whose effect would further move these changes towards positive values. Its effect on past Mediterranean sea level rise has been estimated about 1.2 mm per year during the period 1948–2000 (Calafat et al., 2010). If it will persist in the next decades, this past trend would add about 6 cm in 50 years, increasing the probability of water level reaching values substantially higher than now during storms. The future effect of mass addition on water level extremes can be estimated by adding an uniform sea level increase along the whole Mediterranean coast to water level maxima. Fig. 9 shows the fraction

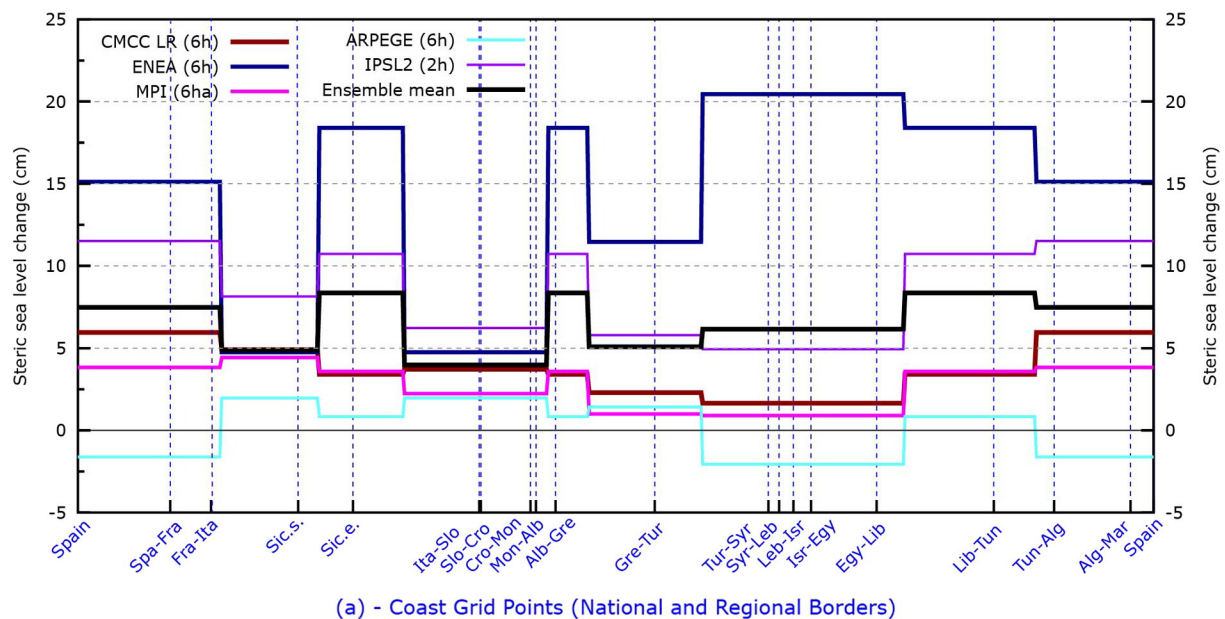


Fig. 7. change of steric sea level (cm) along the Mediterranean coast. Note that the steric sea level is computed as average value in 6 sub-basins: western Mediterranean, Tyrrhenian Sea, Adriatic Sea, Central Mediterranean, Aegean Sea, Levantine basin. Consequently the steric climate change is uniform along the corresponding parts of the Mediterranean coastline.

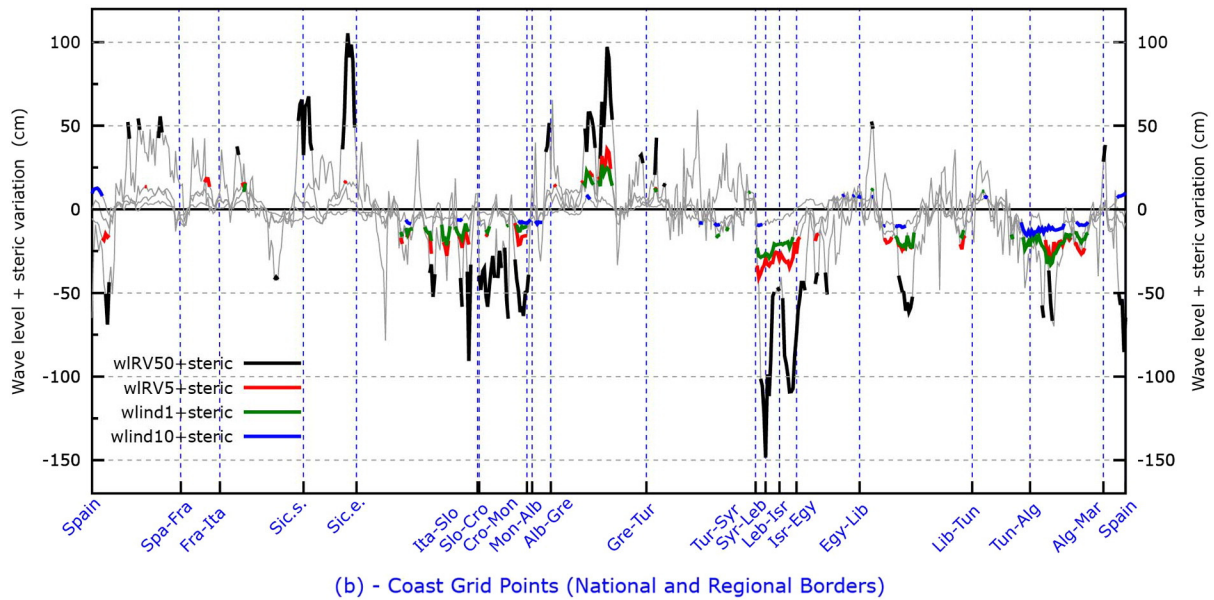


Fig. 8. spatial distribution of the change of max value reached by water during a storm including the effect of surges, waves and steric variation. Only the weighted ensemble mean is shown. Thick parts of the lines denote statistically significant values. Indicators shown are wlrV1 (average annual maximum), wlrV10 (average 10 largest maxima), wlrV5 and wlrV50 (5 and 50 year water level return values).

of Mediterranean coastline, where the increase/decrease of maximum water level indicators wlrV10, wlrV1, wlrV5, wlrV50 in the period 2021–2050 is statistically significant as function of mass addition (represented as an equivalent mean Mediterranean sea level increase). Without mass addition the fraction of coastline with significant increase(decrease) of water level maxima would be the same shown in Fig. 8. This is represented by the values corresponding to 0 sea level equivalent mass addition in Fig. 9, which shows that in this case the fraction of coastline with a decrease of water level extremes (dashed line) would be larger than that with an increase (continuous line). However, as the mass addition contribution increases the situation reverses and a value of 20 cm would imply that the majority of the coastline would experience a larger hazard level than presently, with a negligible part experiencing a reduction. Mass addition will be produced by melting of continental glaciers, Greenland and Antarctica ice caps. Values are uncertain in the literature. The 5th IPCC assessment report (Church et

al., 2013) summarizes this contribution with values in the range $4 \div 23$ cm, $4 \div 21$ cm, $-5 \div 13$ cm for continental glaciers, Greenland and Antarctica, respectively, at the end of the 21st century depending on models and scenarios. An inclusion of such mass additions in this study on extreme water levels is made difficult by these large uncertainties and the different time scale adopted here (mid 21st century) and by IPCC (end of 21st century). However, it looks likely that mass addition will be sufficiently large to determine an increase of the hazard posed by extreme water levels during storms along the Mediterranean coast in the next decades.

5. Conclusions

This study has analyzed the maximum water level that will be reached during a storm along the Mediterranean coastline accounting for future changes of wave height, storm surges and steric effects. The

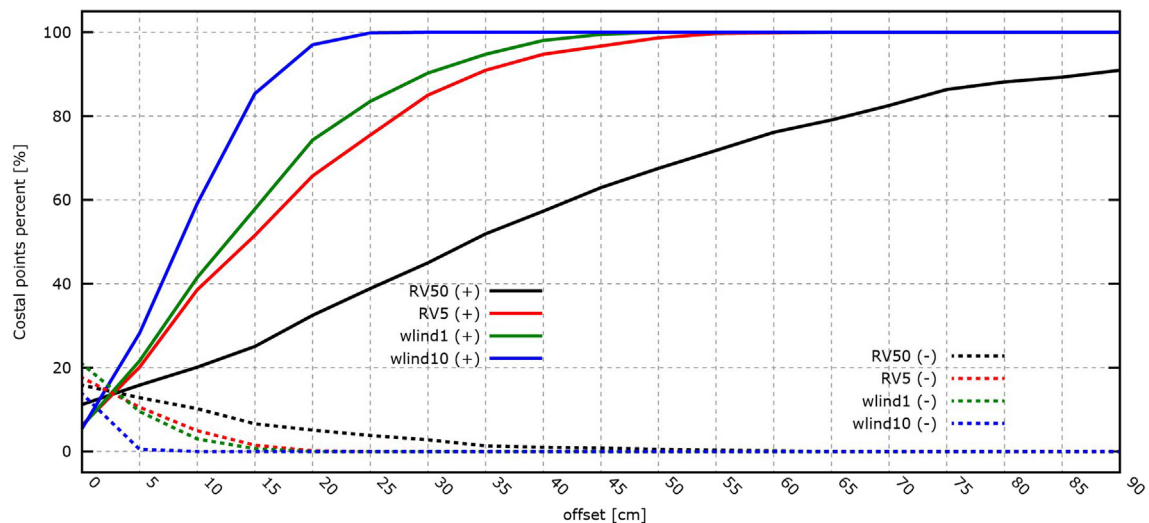


Fig. 9. fraction of Mediterranean coastline (given as fraction of the total number of coastal points in the HYPSE model grid) with a significant increase/decrease (continuous/dashed lines) of the indicators wlrV10 (average 10 largest maxima, blue lines), wlrV1 (average annual maximum, green lines), wlrV5 and wlrV50 (5 and 50 year water level return values, red and black lines) in the period 2021–2050. Changes are computed as function of mass addition, which is represented as an equivalent mean Mediterranean sea level increase(x-axis, cm). (For interpretation of the references to colour in this figure legend, the reader is referred to the web version of this article.)

analysis considers the A1B scenario and the 30-year long period 2021–2050 which is compared to the period 1971–2000.

This paper has first considered only the effect of marine storminess, that is the changes of future maximum water levels that is reached during a storm due to changes of maximum wave amplitude and storm surge. Different levels of extremes have been considered: future percent decrease is similar considering the $wlind10$, $wlind1$, $wlrv5$ indicators, which would imply that the reduction will be larger in absolute value for more rare event than for moderate extremes. The climate change of $wlrv50$ has a more irregular distribution than that of other indicators and presents a large significant increase along the coast of Spain and Greece.

Regional steric effects on sea level are included considering a set of regional climate model simulations including the feedback of the Mediterranean Sea circulation on the atmosphere. Estimates of the steric future increment suggest a range varying with the basins from 4 (for the relatively shallow Adriatic Sea) to 14 cm in 50 years for the model ensemble mean.

Consequently two contrasting regional factors are affecting future water level maxima along the Mediterranean coast: reduction of storminess and increase of water volume. Their superposition suggests that the future change of the overall maximum water level will be mostly not significant along the Mediterranean coast, negative in the Adriatic Sea and along the coast of the Middle East, positive at the coast of Spain, at the coast of Sicily and along both the Ionian and Aegean sectors of the coast of Greece. This pattern is maintained, but amplified, considering events with a multidecadal return time (e.g. $wlrv50$).

Note that the changes for indicators such as $wlind1$, $wlind10$, $wlrv5$ are in the range ± 25 cm, so that land subsidence (not included in this study) will be an essential factors for the effect of water level extremes at the coast at local scale. Further, future water levels will be affected by mass addition entering the Mediterranean Sea through the Gibraltar Strait. The importance of this further factor is uncertain, but it appear likely that it will be sufficiently large to substantially affect the future distribution of water level maxima and increase the intensity of the hazards along the Mediterranean coast already by the mid 21st century.

Acknowledgements

This study has been partially supported by the EU-fp7 RISES-AM project and by the Italian GEMINA project (MIUR/MATTM n. 232/2011).

References

- Amante, C., Eakins, B.W., 2009. ETOPO1 1 arc-minute global relief model: procedures, data sources and analysis. NOAA Technical Memorandum NESDIS NGDC-24 (19 pp.).
- Battjes, J.A., Groenendijk, H.W., 2000. Wave height distributions on shallow foreshores. *Coast. Eng.* 40, 61–182. [http://dx.doi.org/10.1016/S0378-3839\(00\)00007-7](http://dx.doi.org/10.1016/S0378-3839(00)00007-7).
- Battjes, J.A., Janssen, J.P.F.M., 1978. Energy loss and set-up due to breaking of random waves. *Proc. 16th Int. Conf. Coastal Eng., ASCE (1978)*, pp. 569–588.
- Calafat, F.M., Marcos, M., Gomis, D., 2010. Mass contribution to Mediterranean Sea level variability for the period 1948–2000. *Glob. Planet. Chang.* 73 (3–4), 193–201.
- Carillo, A., Sannino, G., Artale, V., Ruti, P.M., Calmanti, S., Dell'Aquila, A., 2012. Steric sea level rise over the Mediterranean Sea: present climate and scenario simulations. *Clim. Dyn.* 39, 2167–2184.
- Church, J.A., Clark, P.U., Cazenave, A., Gregory, J.M., Jevrejeva, S., Levermann, A., Merrifield, M.A., Milne, G.A., Nerem, R.S., Nunn, P.D., Payne, A.J., Pfeffer, W.T., Stammer, D., Unnikrishnan, A.S., 2013. Sea Level Change. In: Stocker, T.F., Qin, D., Plattner, G.-K., Tignor, M., Allen, S.K., Boschung, J., Nauels, A., Xia, Y., Bex, V., Midgley, P.M. (Eds.), *Climate Change 2013: The Physical Science Basis Contribution of Working Group I to the Fifth Assessment Report of the Intergovernmental Panel on Climate Change*. Cambridge University Press, Cambridge, United Kingdom and New York, NY, USA.
- Conte, D., Lionello, P., 2013. Characteristics of large positive and negative surges in the Mediterranean Sea and their attenuation in future climate scenarios. *Glob. Planet. Chang.* 111, 159–173. <http://dx.doi.org/10.1016/j.gloplacha.2013.09.006> (ISSN 0921-8181).
- Déqué, M., Pledelievre, J.P., 1995. High-resolution climate simulation over Europe. *Clim. Dyn.* 11, 321–339.
- Elizalde, A., Sein, D., Mikolajewicz, U., Jacob, D., 2010. Regional atmosphere-ocean-hydrology coupled climate model. Max Planck Institute for Meteorology Technical Report (5pp, available at) http://www.rem0-rcm.de/fileadmin/user_upload/rem0/UBA/pdf/TechnicalReport.pdf.
- Goda, Y., 1978. The observed joint distribution of periods and heights of sea waves. *Proc. 16th Coastal Eng. Conf. vol. 2*, pp. 227–246.
- Goda, Y., 2008. Overview on the applications of random wave concept in coastal engineering. *Proc. Jpn. Acad. Ser. B Phys. Biol. Sci.* 84, 374–385. <http://dx.doi.org/10.2183/pjab/84.374>.
- Gualdi, S., Somot, S., Li, L., Artale, V., Adani, M., Bellucci, A., Braun, A., Calmanti, S., Carillo, A., Dell'Aquila, A., Déqué, M., Dubois, C., Elizalde, A., Harzallah, A., Jacob, D., L'Hévéder, B., May, W., Oddo, P., Ruti, P., Sanna, A., Sannino, G., Scoccimarro, E., Sevault, F., Navarra, A., 2013. The CIRCE simulations: a new set of regional climate change projections performed with a realistic representation of the Mediterranean Sea. *Bull. Am. Meteorol. Soc.* 94, 65–81.
- Jordà, G., Gomis, D., 2013a. On the interpretation of the steric and mass components of sea level variability: the case of the Mediterranean basin. *J. Geophys. Res. Oceans* 118, 953–963.
- Jordà, G., Gomis, D., 2013b. Reliability of the steric and mass components of Mediterranean Sea level as estimated from hydrographic gridded products. *Geophys. Res. Lett.* 40 (14), 3655–3660.
- Jordà, G., Gomis, D., Álvarez-Fanjul, E., Somot, S., 2012. Atmospheric contribution to Mediterranean and nearby Atlantic Sea level variability under different climate change scenarios. *Glob. Planet. Chang.* 80, 198–214.
- Li, L.Z.X., 2006. Atmospheric GCM response to an idealized anomaly of the Mediterranean Sea surface temperature. *Clim. Dyn.* 27, 543–552.
- Li, L., Casado, A., Congedi, L., Dell'Aquila, A., Dubois, C., Elizalde, A., Hévéder, B.L., Lionello, P., Sevault, F., Somot, S., Ruti, P., Zampieri, M., 2012. Modeling of the Mediterranean climate system. In: Lionello, P. (Ed.), *The Climate of the Mediterranean Region From the Past to the Future*. Elsevier (Netherlands), Amsterdam. ISBN: 9780124160422, pp. 419–448.
- Lionello, P., Giorgi, F., 2007. Winter precipitation and cyclones in the Mediterranean region: future climate scenarios in a regional simulation. *Adv. Geosci.* 12, 153–158.
- Lionello, P., Sanna, A., 2005. Mediterranean wave climate variability and its links with NAO and Indian Monsoon. *Clim. Dyn.* 25, 611–623.
- Lionello, P., Mufato, R., Tomasin, A., 2005. Sensitivity of free and forced oscillations of the Adriatic Sea to sea level rise. *Clim. Res.* 29, 23–39.
- Lionello, P., Bhend, J., Buzzi, A., Della-Marta, P.M., Krichak, S., Jansà, A., Maheras, P., Sanna, A., Trigo, I.F., Trigo, R., 2006. Cyclones in the Mediterranean region: climatology and effects on the environment. In: Lionello, P., Malanotte-Rizzoli, P., Boscolo, R. (Eds.), *Mediterranean Climate Variability*. Elsevier (Netherlands), Amsterdam, pp. 325–372.
- Lionello, P., Boldrin, U., Giorgi, F., 2008a. Future changes in cyclone climatology over Europe as inferred from a regional climate simulation. *Clim. Dyn.* 30, 657–671. <http://dx.doi.org/10.1007/s00382-007-0315-0>.
- Lionello, P., Cogo, S., Galati, M.B., Sanna, A., 2008b. The Mediterranean surface wave climate inferred from future scenario simulations. *Glob. Planet. Chang.* 63, 152–162. <http://dx.doi.org/10.1016/j.gloplacha.2008.03.004>.
- Longuet-Higgins, M.S., 1975. On the joint distribution of the periods and amplitudes of sea waves. *J. Geophys. Res.* 80 (18), 2688–2693.
- Marcos, M., Tsimplis, M., 2008. Comparison of results of AOGCMs in the Mediterranean Sea during the 21st century. *J. Geophys. Res.* 113 (C12). <http://dx.doi.org/10.1029/2008JC004820>.
- Marcos, M., Calafat, F.M., Llovel, W., Gomis, D., Meyssignac, B., 2011a. Regional distribution of steric and mass contributions to sea level changes. *Glob. Planet. Chang.* 76 (3), 206–218.
- Marcos, M., Jordà, G., Gomis, D., Pérez, B., 2011b. Changes in storm surges in southern Europe from a regional model under climate change scenarios. *Glob. Planet. Chang.* 77 (3), 116–128.
- Marcos, M., Jordà, G., Gomis, D., Holgate, S., Tsimplis, M., Barnier, B., 2011c. Report on the workshop unresolved issues in Mediterranean Sea level research, Palma de Mallorca, 30 May–1 June. Available from: <http://imedea.uib-csic.es/proyecto/sealevel/Finalreport-archivos/FINAL-REPORT-v2.pdf>.
- Nelson, R.C., 1994. Depth limited design wave heights in very flat regions. *Coast. Eng.* 23, 43–59.
- Nicholls, R.J., Hoozemans, F.M.J., 1996. The Mediterranean: vulnerability to coastal implications of climate change. *Ocean Coast. Manag.* 31, 105–132.
- Oddo, P., Adani, M., Pinardi, N., Fratianni, C., Tonani, M., Pettenuzzo, D., 2009. A nested Atlantic-Mediterranean Sea general circulation model for operational forecasting. *Ocean Sci. Discuss.* 5, 461–473.
- Scarcia, L., Lionello, P., 2013. Global and regional factors contributing to the past and future sea level rise in the northern Adriatic Sea. *Glob. Planet. Chang.* 106, 51–63. <http://dx.doi.org/10.1016/j.gloplacha.2013.03.004>.
- Somot, S., Sevault, F., Déqué, M., Crépon, M., 2008. 21st century climate change scenario for the Mediterranean using a coupled atmosphere-ocean regional climate model. *Glob. Planet. Chang.* 63 (2–3), 112–126. <http://dx.doi.org/10.1016/j.gloplacha.2007.10.003>.
- Tsimplis, M.N., Rixen, M., 2002. Sea level in the Mediterranean Sea: the contribution of temperature and salinity changes. *Geophys. Res. Lett.* 29 (23), 2136. <http://dx.doi.org/10.1029/2002GL015870>.
- Tsimplis, M.N., Álvarez-Fanjul, E., Gomis, D., Fenoglio-Marc, L., Pérez, B., 2005. Mediterranean Sea level trends: atmospheric pressure and wind contribution. *Geophys. Res. Lett.* 32 (20).
- Tsimplis, M., Marcos, M., Somot, S., Barnier, B., 2008. Sea level forcing in the Mediterranean Sea between 1960 and 2000. *Glob. Planet. Chang.* 63 (4), 325–332.
- WAMDI group, Hasselmann, S., Hasselmann, K., Bauer, E., Janssen, P.A.E.M., Komen, G., Bertotti, L., Lionello, P., Guillaume, A., Cardone, V.C., Greenwood, J.A., Reistad, M., Zambresky, L., Ewing, J.A., 1988. The WAM model – a third generation ocean wave prediction model. *J. Phys. Oceanogr.* 18, 1776–1810.
- Zappa, G., Shaffrey, L.C., Hodges, K.J., Sanson, P.G., Stephenson, D.B., 2013. A multimodel assessment of future projections of north atlantic and european extratropical cyclones in the cmip5 climate models. *J. Clim.* 26, 5846–5862.